University of Padua, Department of Chemical Science
BSc Thesis in Materials Science

Synthesis and Characterization of Vanadium Dioxide (VO_2) Thin Films via Magnetron Sputtering for the Analysis of Metal-Insulator Phase Transitions

Pietro Lorenzi
ID 2102479

Supervisor
Prof. Giovanni Mattei
University of Padova

Academic Year 2025-2026

To my parents
and friends

Contents

Abstract

Vanadium Dioxide VO_2 is a transition metal oxide that characterized by a sharp, reversible, first-order Metal-Insulator Transition (MIT) at 68°C. The transition is accompanied by a structural transformation from a monoclinic (M1) to a rutile (R) crystal phase. This thesis reports on the synthesis and characterization of four 120 nm VO_2 thin films grown on silicon and silica substrates by DC reactive magnetron sputtering. Two of these films subsequently underwent post-deposition thermal annealing at 490°C in a nitrogen atmosphere to promote crystallization and achieve the correct stoichiometry. Surface morphology was characterized through profilometry, Scanning Electron Microscopy (SEM), and Atomic Force Microscopy (AFM). The results indicated an average grain diameter of 52 nm, a surface roughness of 3.1 nm, and a film thickness of 125 nm. Structural characterization via Grazing-Incidence X-Ray Diffraction (GIXRD) and Raman spectroscopy confirmed the formation of the monoclinic M1 crystalline phase at room temperature and rutile R above the transition temperature. The optical transmittance of the films was measured by UV-Vis-NIR spectrophotometry, and from spectroscopic ellipsometry, the refractive index and extinction coefficients were extracted through a three-oscillator Lorentz model fit. The phase transition was studied by heating the samples and measuring both the optical transmittance at 1550 nm and 800 nm, and the shift of the GIXRD diffraction peak at 27.9°, as a function of temperature across a 30–90°C range. Both techniques revealed a clear hysteresis cycle, with heating and cooling transition temperatures of approximately 67°C and 57°C respectively from optical spectrophotometer, and 69°C and 60°C from the XRD. The comparison between the two results highlights the different approaches of the two techniques and the different observed material properties (structural for the x-rays and electronic for the optical spectroscopy).

Sommario

Il biossido di Vanadio VO_2 è un ossido di metallo di transizione caratterizzato da una rapida e reversibile transizione Metallo-Isolante (MIT) del primo ordine a 68°C. La transizione è accompagnata da una trasformazione da struttura monoclina (M1) isolante a una tetragonale (R) metallica. Questo lavoro di tesi presenta il processo di sintesi e caratterizzazione di 4 film sottili di 120 nm di VO_2 depositati su substrati di silice e silicio tramite DC magnetron sputtering reattivo. Su due campioni è stato eseguito un trattamento termico a 490°C in atmosfera di azoto per favorire la cristallizzazione e la corretta stechiometria. La morfologia è stata caratterizzata tramite profilometria, Microscopio elettronico a scansione (SEM) e microscopio a forza atomica (AFM). I risultati hanno indicato uno spessore del film di 125 nm, una rugosità di 3.1 nm e un diametro medio dei grani di 52 nm. L'analisi strutturale eseguita tramite Grazing Incidence X-Ray Diffraction (GIXRD) e spettroscopia Raman ha confermato la formazione della fase monoclina a temperatura ambiente e di quella tetragonale sopra la temperatura di transizione. La trasmittanza ottica è stata misurata con spettrofotometro Uv-vis-nir e, tramite ellissometria con fit modellato con tre oscillatori di Lorentz, sono stati ricavati indice di rifrazione e coefficiente di estinzione. La transizione di fase è stata studiata scaldando i campioni in un ciclo da 30-90°C e misurando la trasmittanza a 1550 nm, 800 nm e lo shift del picco di diffrazione a 27.9°. Entrambe le tecniche hanno prodotto un chiaro ciclo di isteresi con temperatura di transizione in salita e discesa di 67°C e 57°C rispettivamente per le misure ottiche e 69°C e 60°C per i raggi X. Il confronto tra le due ha evidenziato i due diversi approcci e parti del materiale osservato (struttura atomica per i raggi X e struttura elettronica per lo spettrofotometro).

1 Introduction

1.1 Background

Vanadium (IV) Dioxide (VO_2) is a transition metal oxide, known for its reversible MIT (Metal insulator Transition) at 68°C and its large number of possible applications (see Figure 1.1). The transition is characterized by a change in the crystal structure from a low temperature insulating monoclinic (M1) to a high temperature metallic rutile (R) phase.[1]

The reason for the strong interest in this material is that its sharp, first-order transition causes a profound change across different physical properties [2, 3]:

1. The material changes from transparent to reflective in the NIR part of the spectrum
2. Electrical conductivity increases by several orders of magnitude.
3. Thermal conductivity increases substantially.

The physical origin of the transition is currently under debate. Two competing mechanisms are proposed: a lattice driven Peierls transition or a Mott-Hubbard electron driven transition. Current studies suggest both mechanisms play a role although the exact weight of each one is yet to be determined [4].

The interesting physical changes of the transition offer a large variety of applications, such as thermochromic efficient smart windows [5] and ultrafast optical switches [6, 7].

In order to fully optimize and tune parameters such as transition temperature, broadness, and hysteresis to meet specific requirements, thorough studies of Deposition techniques such as Magnetron Sputtering [9], CVD [10] and Sol-Gel [11], substrate type effects [12, 13] and doping effects [14, 15] have been carried out.

1.2 Project description and methods

The aim of the present project was to gather hands on experience on all the steps from the synthesis to the characterization of a VO_2 thin film and the study of its phase change. All the experimental activities were conducted at the NanoStructures Group (NSG) of the Department of Physics and Astronomy at the University of Padova. The first part involved the film synthesis by magnetron sputtering on silica and silicon substrates to learn how different deposition parameters impacted the final result. The objective of the characterization part was to give an overview of many different techniques to examine the material from various points of view. The activities were divided into morphological

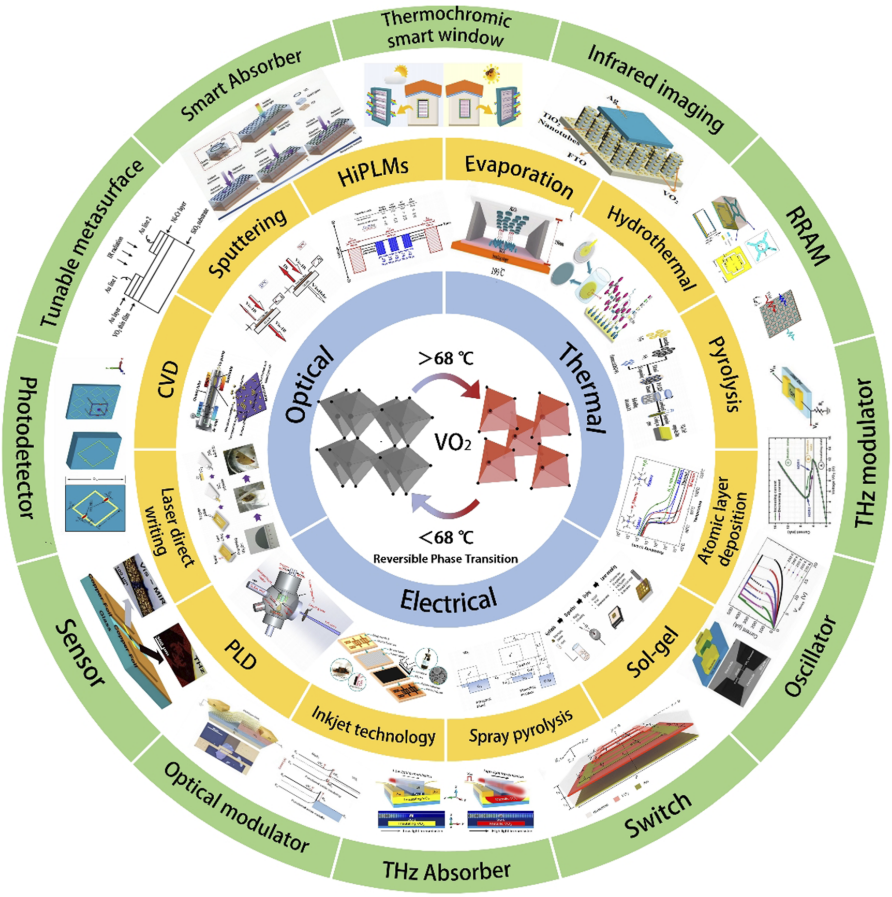

Figure 1.1: Scheme of some of the possible applications of VO_2 thin films. Reprinted from [8]

(Profilometry, SEM, AFM), structural (GIXRD, Raman spectroscopy), and optical (Uv-vis spectroscopy, Ellipsometry) analysis. The last part involved the study of phase change properties by looking at the transition hysteresis from two points of view. GIXRD and Uv-vis measurements were conducted *in-situ* during the heating and cooling of the sample, and the resulting hysteresis curve with its width and temperature was derived.

1.3 Objectives of the Thesis

The primary objective of this thesis is to provide a complete, hands-on overview of the full workflow involved in the fabrication and study of a functional thin-film material, from synthesis to advanced characterization. Specifically, the work aims to:

1. Synthesize 120 nm VO_2 thin films on Silica and Silicon, and ensure the correct stoichiometry via thermal annealing after the deposition (Chapter 2).
2. Characterize the morphology of the film via Profilometry, SEM and AFM to obtain the thickness, surface roughness and grain distribution (Chapter 3).
3. Confirm the ambient temperature M1 crystalline structure by examining the peaks of Raman spectroscopy and GIXRD (Chapter 4).
4. Observe the transmittance and dielectric function properties via Uv-vis spectroscopy and Ellipsometry (Chapter 5).
5. Study and quantify the thermal hysteresis of the Metal-Insulator Transition by track-

ing both the optical transmittance and the structural diffraction signal as a function of temperature, and compare the results obtained from the two independent techniques (Chapter 6).

2 Synthesis of VO_2 Thin Films

2.1 Substrate Preparation

The VO_2 layers were deposited on two types of substrates: silica glass (Heraeus HSQ100) and silicon. Silicon was employed for structural and morphological characterizations, whereas the transparent silica was utilized for optical measurements. To ensure the complete removal of organic residues and impurities, the substrates were immersed in a piranha solution (a 3:1 volumetric mixture of concentrated H_2SO_4 and 30% H_2O_2) at a temperature of 100 °C for one hour. Following the acid bath, they were rinsed with ultrapure water and dried using a nitrogen gas flux.

2.2 DC Magnetron Sputtering Deposition

The thin films were grown via direct current (DC) reactive magnetron sputtering. A pure vanadium metallic target with a 50 mm diameter, 5 mm height, and 99.9% purity was employed. The substrates were mounted on a symmetrical, three-blade rotating holder placed at a 17 degree tilt from the target.

Initially, the sputtering chamber was evacuated to a high vacuum level of approximately 5×10^{-6} mbar to degas the chamber walls. A flow of 14 sccm of high-purity argon was then introduced, setting the chamber pressure to roughly 10^{-4} mbar. A plasma of argon ions was generated by applying a high negative voltage of 399 V.

For the reactive growth of the oxide film, a small oxygen flow of 1.0 sccm was injected alongside argon. This flow was continuously tuned to maintain the target potential within a range of 390 to 399 V.

2.3 Thermal Annealing Treatment

The films produced directly from the sputtering process were in an amorphous phase. To induce crystallization necessary for the phase transition, a post-deposition thermal treatment was performed in a tube furnace.

The annealing step was conducted in an inert atmosphere with a constant nitrogen flow of 20 nL/h. The temperature was increased at a rate of 250 °C/h up to 490 °C, held for 1 hour , and then ramped down to room temperature. This process successfully yielded polycrystalline VO_2.

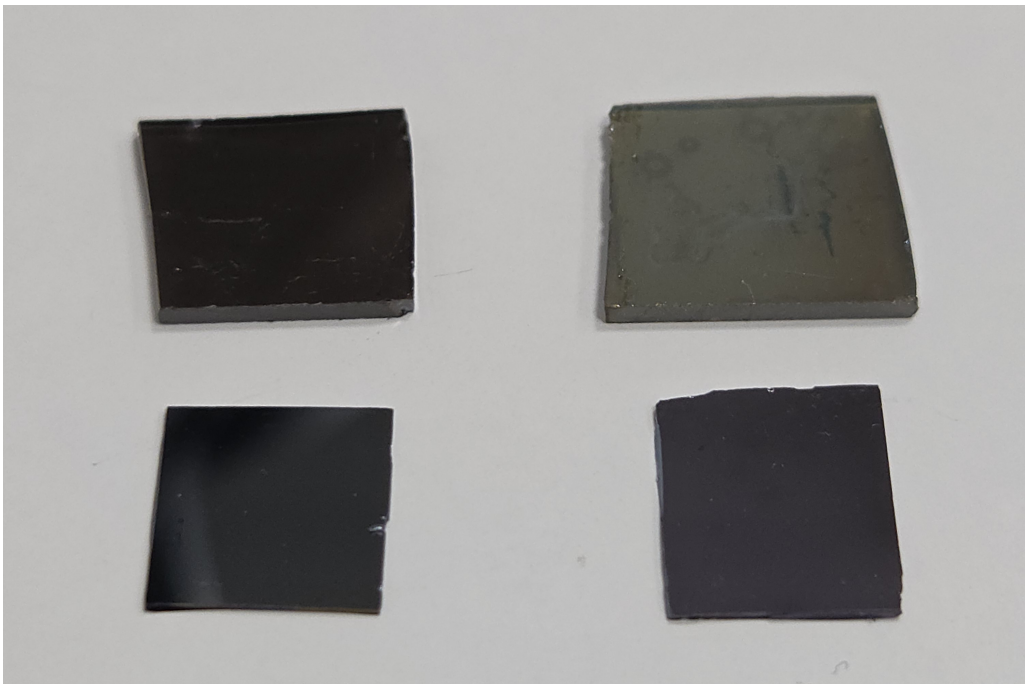

Figure 2.1: Picture of the 4 different prepared samples (SiO_2 on the first row and Si on the bottom row), before the annealing (left), and after the annealing (right)

3 Surface Characterization

3.1 Profilometer analysis

An additional piece of silicon substrate was included in the deposition to be later scanned by a profilometer (KLA Tencor P-17) to ensure the expected thickness. Before the deposition, an alcohol based marker was used to make a cross-shaped mask on the substrate that was later removed to expose the bare wafer and create a step as thick as the film. The machine measures thickness and roughness by passing a stylus over the surface of the sample and recording the vertical movements caused by the contours of the material.

3.2 Scanning Electron Microscopy (SEM)

The surface morphology, grain size, and shape of the VO_2 thin films were investigated using a high-resolution field-emission scanning electron microscope (Zeiss Sigma Gemini HD). The primary electron beam, produced by field emission, interacts with the sample to generate various signals, including back-scattered electrons, secondary electrons, and characteristic X-rays. For the morphological characterization in this study, the images were acquired using an In-Lens detector. This detector specifically collects low-energy secondary electrons generated by inelastic scattering to map the surface topography. To mitigate the electron accumulation caused by dielectric substrates, the SEM images were taken exclusively on the conductive Silicon substrate. Quantitative grain size analysis was conducted on the acquired scans utilizing the ImageJ software equipped with the MorphoLibJ plugin. Following a morphological segmentation procedure to identify grain

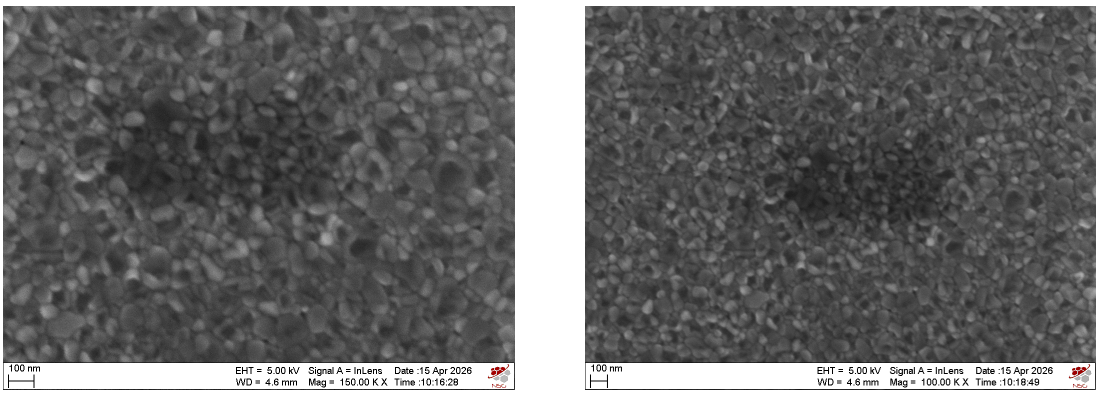

Figure 3.1: SEM images of the VO_2 film on silicon, taken at two different magnifications.

boundaries, the extracted grain areas were statistically analyzed. The area data were fitted to an asymmetric Log-Normal distribution, as in Refs. [16, 17]:

$$f_{\text{Log-Norm}}(x;\mu,\sigma) = \frac{1}{\sigma x\sqrt{2\pi}} \exp\left[-\frac{(\ln x-\mu)^2}{2\sigma^2}\right]. \tag{3.1}$$

where the average grain area is: $\mathcal{A} \equiv e^{\mu+\sigma^2/2}$ with variance $\Delta\mathcal{A} \equiv \sqrt{e^{\sigma^2}-1}\, e^{\mu+\sigma^2/2}$. The resulting average grain diameter D (i.e., the diameter of the circle with the same average area) is calculated as:

$$D = 2\sqrt{\frac{\mathcal{A}}{\pi}}. \tag{3.2}$$

The fit resulted in D = 52 nm with a variance of ΔD = 23 nm.

3.3 Atomic Force Microscopy (AFM)

Surface topography and roughness were further evaluated using an NT-MDT Solver Pro atomic force microscope. The measurements were performed in semi-contact (tapping) mode, wherein the tip is positioned in close proximity to the surface without maintaining continuous physical contact. In this configuration, the cantilever is driven to oscillate near its resonant frequency.

The topography is mapped by monitoring the variations in the cantilever's oscillation frequency caused by tip-sample interactions. This detection is achieved via a laser beam reflecting off the back of the cantilever onto a four-quadrant photodiode matrix. A feedback electronic system continuously utilizes piezoelectric elements to adjust the vertical position during the $x-y$ scan, maintaining the oscillation amplitude at a constant reference setpoint.

Scans were acquired from the VO_2 thin film on silicon, over sampling areas of 2 μm^2 and 4 μm^2 with scanning frequencies of 0.2 Hz and 0.25 Hz, respectively, and a lateral resolution of 250 points per line. The surface roughness, defined as the deviation of the surface from the mean plane, was subsequently extracted from the AFM images using Gwyddion software. The grain height distribution was found to be a perfectly symmetrical Gaussian, and the average roughness value was found to be 3.1 nm.

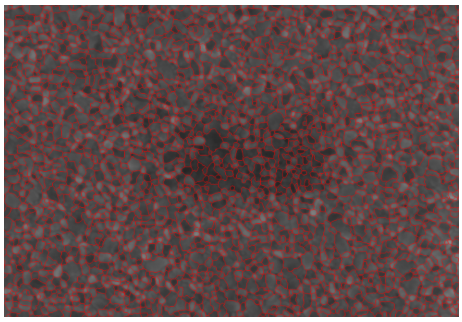

Figure 3.2: SEM image of the VO_2 film with the *Imagej* morphological segmentation overlaid.

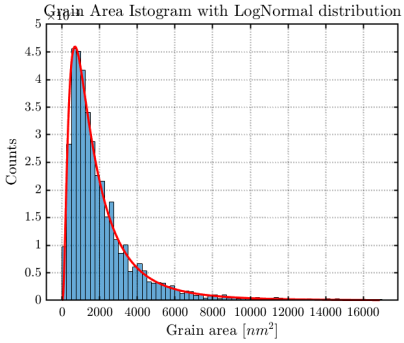

Figure 3.3: Log-normal distribution histogram of the grains area.

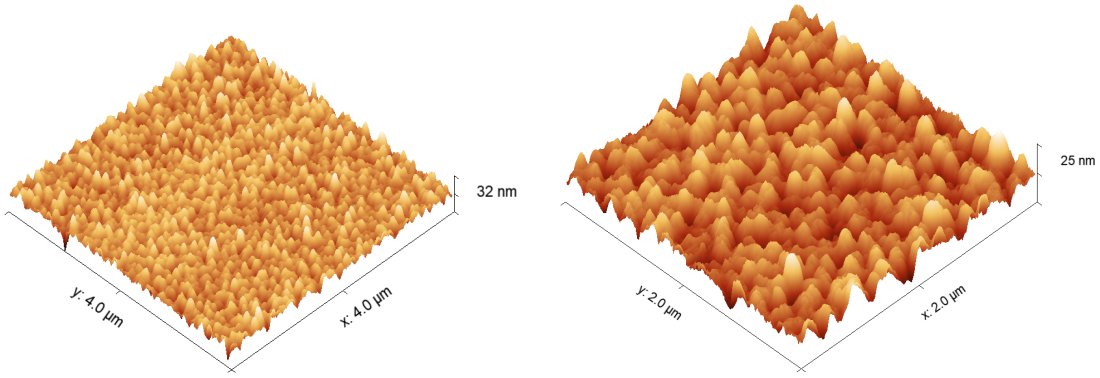

Figure 3.4: AFM scans of the VO_2 film on silicon, 2 μm^2 sampling area on the right and 4 μm^2 on the left.

4 Structural Characterization

4.1 Grazing-Incidence X-Ray Diffraction (GIXRD)

To investigate the crystalline structure and phase transitions of the VO_2 thin films, Grazing-Incidence X-Ray Diffraction (GIXRD) was employed. Unlike standard X-ray diffraction, the grazing incidence geometry utilizes a very small X-ray beam incidence angle ω with respect to the sample surface (typically below $1°$) to limit the penetration depth into the material. This ensures that the acquired diffraction pattern is predominantly generated by the thin surface layer rather than the substrate below.

The structural measurements were performed using a Panalytical X'Pert Pro diffractometer equipped with a Cu $K\alpha$ radiation source ($\lambda = 0.15406$ nm). The experimental setup was configured with a fixed incidence angle $\omega = 0.5°$, while the scattering angle 2θ was scanned in the $20° \div 60°$ range. To study the thermally induced semiconductor-to-metal transition *in situ*, the samples were placed on an Anton Paar DHS900 heating stage (capable of reaching up to 900°C), with the surface temperature continuously monitored by a thermocouple. The measurements were conducted in a range of temperatures between 30°C and 90°C with a step of 3°C.

The diffraction peaks Miller indices were identified by running an XRD simulation on the software VESTA with crystallographic data taken from the materials project database,[18] for the monoclinic phase and [19] for the tetragonal phase.

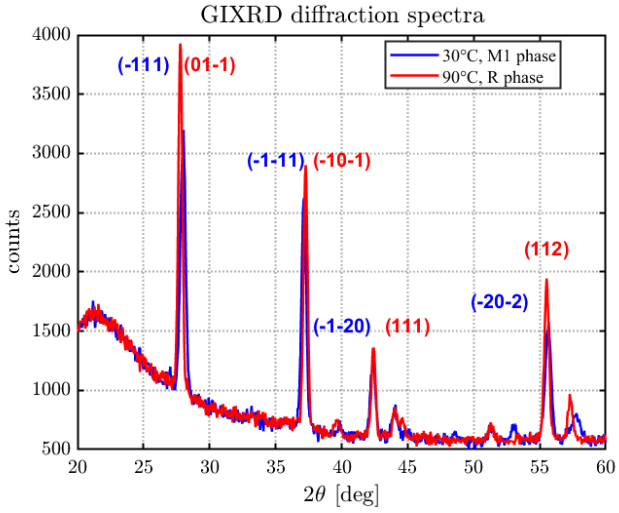

Figure 4.1: GIXRD spectra at 30 and 90°C

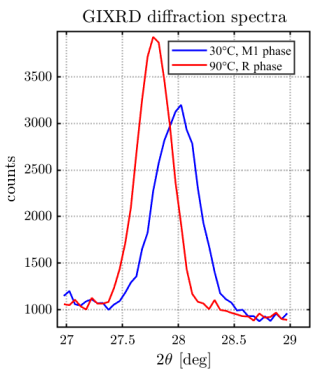

Figure 4.2: Focus on the 27.9° peak (which will be used for the hysteresis)

4.2 Raman Spectroscopy

Complementary structural analysis was performed using Raman spectroscopy, a technique based on the inelastic scattering of photons to detect the vibrational modes of the crystal lattice.

The Raman spectra were acquired with a HORIBA XploRA PLUS microscope operating in a backscattering configuration. A laser source with a wavelength of 638 nm was used for the excitation. The optical power delivered to the specimen was carefully tuned to prevent localized overheating or structural degradation of the vanadium dioxide layer.

This technique is highly effective for identifying the low-temperature monoclinic (M1) phase of VO_2 on the silicon substrate. The acquired spectra reveal characteristic phonon peaks: the prominent peak at 521 cm^{-1} represents the response of the silicon substrate. The low-frequency modes (specifically those located at 195.7 and 224.7 cm^{-1}) are associated with the vibrational motion involving the V-V dimer bonds[16]. The small peaks at 146.2, 262.3, 309.4 and 387.2 are attributed to vibrations of V-O bonds[16].

For the R phase the Raman spectrum is almost structureless,[16] so it has not been reported.

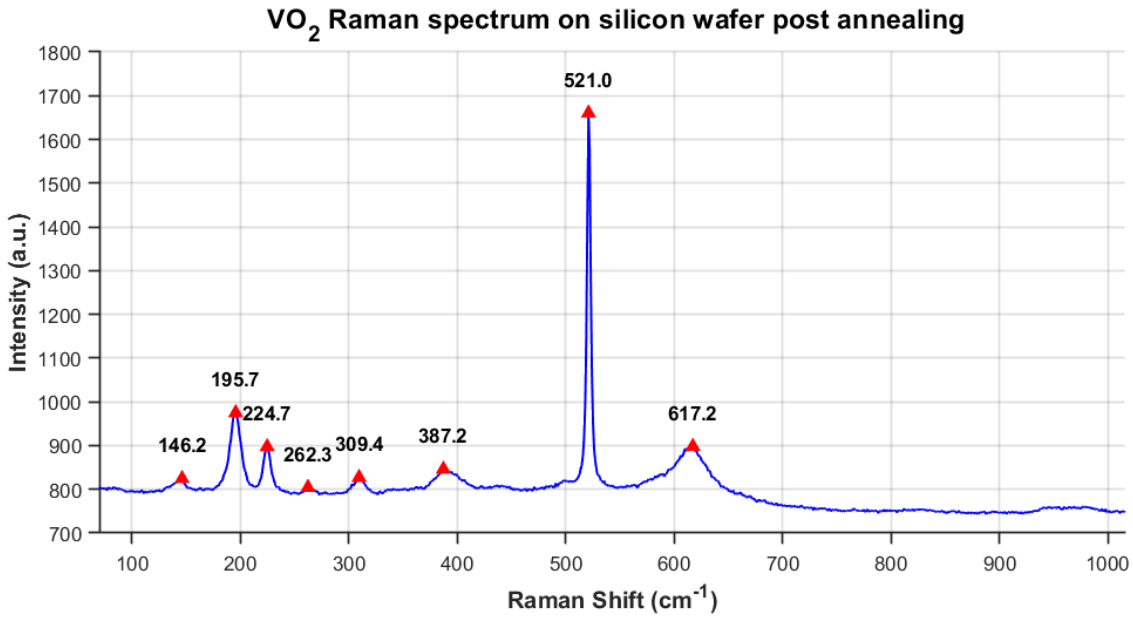

Figure 4.3: Raman spectra of the M1 phase at ambient temperature.

5 Optical Characterization

5.1 UV-Vis-NIR Spectrophotometry

To evaluate the optical transmittance of the fabricated thin films, measurements were performed using a JASCO V-670 UV-Vis-NIR spectrophotometer. The instrument operates in a double-beam configuration, where one beam passes through the sample and the other is directed to a reference detector, allowing the transmittance to be determined by comparing the two collected intensities. To isolate the optical contribution of the VO_2 layer, the transmittance of a bare silica substrate was initially measured and subtracted by the software as a baseline.

The transmittance spectra were recorded across a spectral range from 400 nm to 1700 nm, using a sampling pitch of 1.0 nm and a scanning speed of 400 nm/min. During the measurements, the film was mounted on a heatable sample holder equipped with a controller and a thermocouple that monitored the temperature directly on the surface of the VO_2 layer with a precision of 1 °C. The heater was connected to an external computer that,

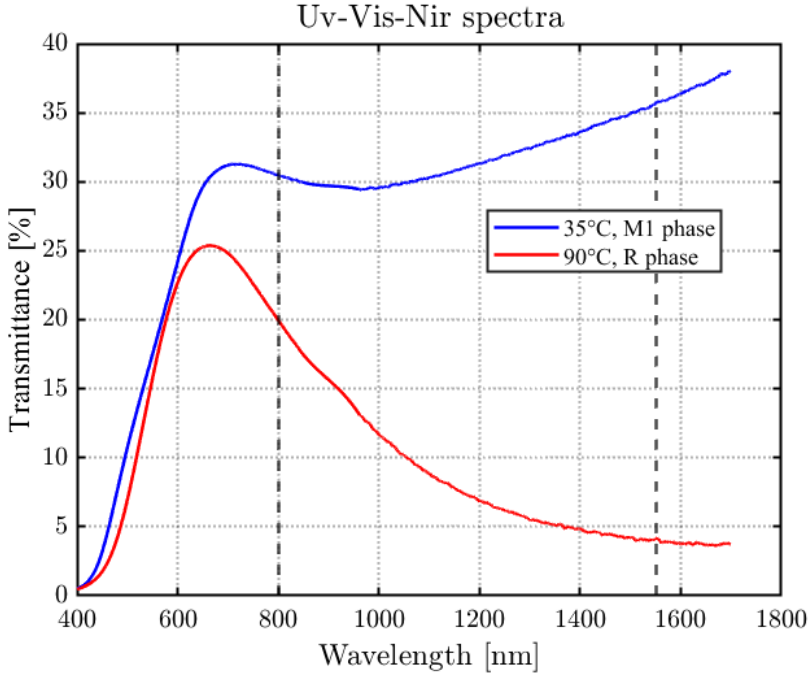

Figure 5.1: Uv-vis spectra of the VO_2 $M1$ and R phases. Gray dashed lines indicates the wavelengths (λ_1 = 800 nm and λ_2=1550 nm) at which the optical hysteresis cycles were calculated.

upon being manually programmed, automatically completed the measurement cycle. Figure 5.1 reports the transmittance for the $M1$ and R phases. Two specific wavelengths are selected for specific applications of the VO_2 thin films: λ_1 = 800 nm for the coupling with quantum emitters for nanolasers and and λ_2=1550 nm for single photon sources in the telecom band.

5.2 Spectroscopic Ellipsometry

The refractive index and the extinction coefficient of the VO_2 were investigated using a J.A. Woollam VASE variable-angle spectroscopic ellipsometer, which covers a broad spectral range from 190 nm to 3200 nm. The system emits a probe beam with known s and p polarization onto the surface of the sample and measures the modified polarization state after the beam is reflected. This interaction is quantified via the complex Fresnel reflection coefficients ($\tilde{R}_s$ and $\tilde{R}_p$), which define the fundamental ellipsometric equation:

$$\tilde{\rho} \equiv \frac{\tilde{R}_p}{\tilde{R}_s} = \tan\Psi e^{i\Delta} \tag{5.1}$$

where $\tan\Psi$ represents the magnitude ratio of the reflection coefficients, and Δ is the phase difference between the p- and s-polarized components. These ellipsometric parameters were acquired at ambient temperature over a spectral window from 400 nm to 1700 nm.

To extract the complex refractive index (with the convention $\tilde{n} = n - ik$) from the raw experimental data, a multi-layer model was constructed within the VASE software consisting of three layers:

1. A 0.5 mm-thick silicon (Si) substrate;
2. A VO_2 layer with an initial trial thickness derived from contact profilometry (126 nm) and temporary dielectric function parameters taken from the literature;
3. A surface effective layer accounts for the macroscopic topography and surface roughness measured via AFM (3.1nm).

In the final refinement step, the temporary literature values of the VO_2 layer were replaced by a General Oscillator (`genosc.mat`) layer. This framework treats the film as a Lorentz medium, modeling the total dielectric function as a series of localized and free-carrier oscillators that automatically satisfy the Kramers-Kronig consistency conditions.

The exact parametrization used to describe the complex dielectric function (using the convention $\epsilon = \epsilon_1 - i\epsilon_2$) was composed by an offset term (ϵ_∞) and three distinct Lorentz oscillators:

$$\epsilon_{M1}(E) = \epsilon_\infty + \sum_{j=1}^{3} \frac{f_j L_j^2}{L_j^2 - E^2 - i\gamma_j E} \tag{5.2}$$

Oscillator	**Amplitude f_j**	**Centroid L_j (eV)**	**Broadening γ_j (eV)**
Lorentz 1	1.526	1.307	0.909
Lorentz 2	0.862	3.003	0.680
Lorentz 3	4.436	4.346	2.062

Table 5.1: Fitted Lorentz oscillators coefficients, the offset value is ϵ_∞=2.614

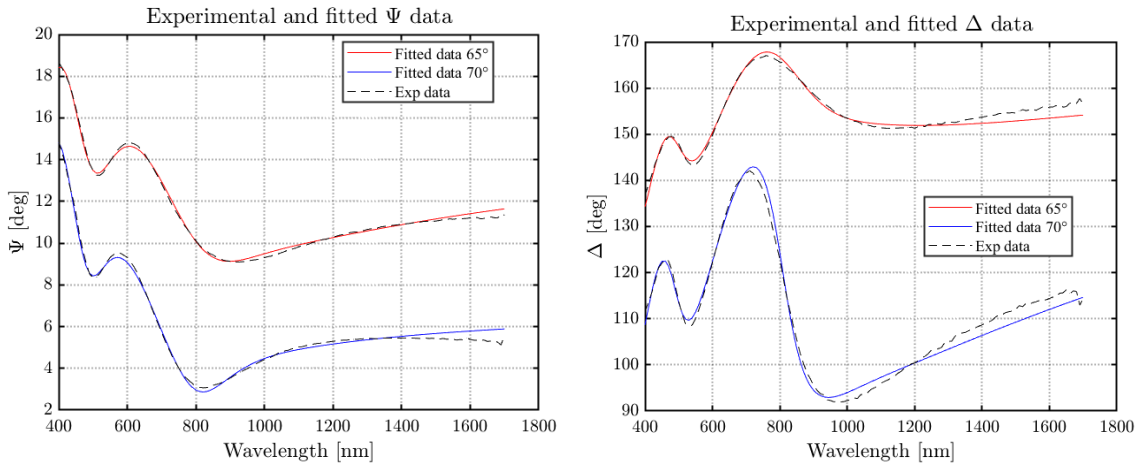

Figure 5.2: Ψ and Δ experimental data and Lorentz oscillator fit results

where f_j, L_j, and γ_j represent the amplitude, the energy centroid, and the broadening parameter of each j-th oscillator, respectively. The results of the fit for the $M1$ phase are reported in Table 5.1. Figure 5.2 reports a comparison between the measured Ψ and Δ values obtained at different incidence angles (65° and 70°).
Once the fit was completed, the values for the n and k coefficients were obtained directly from the software.

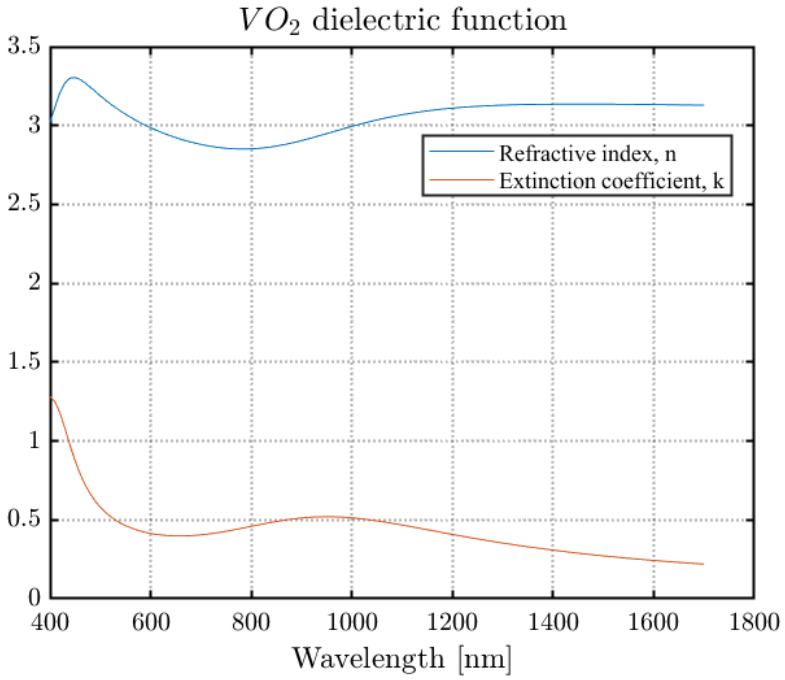

Figure 5.3: n and k coefficients of the dielectric function for the $M1$ phase as a function of the wavelength.

6 Phase Change Hysteresis Cycles

Compared to bulk materials, vanadium dioxide thin films typically exhibit a broader phase transition. The resulting thermal hysteresis loop can be thoroughly investigated by characterizing changes in the macroscopic optical properties, such as transmission at the NIR range [20], or by tracking the evolution of specific Bragg reflections within the X-ray diffraction patterns [3, 21].

6.1 Optical Transmittance Hysteresis

To analyze the optical hysteresis behavior, the transmittance of the films is monitored at two fixed wavelengths of 1550 and 800 nm as a function of temperature, where the temperature interval was 30-90°C with a step of 3°C.

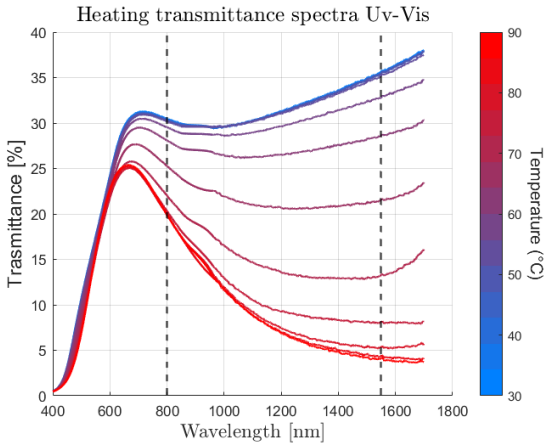

Figure 6.1: Heating evolution of the transmittance spectra

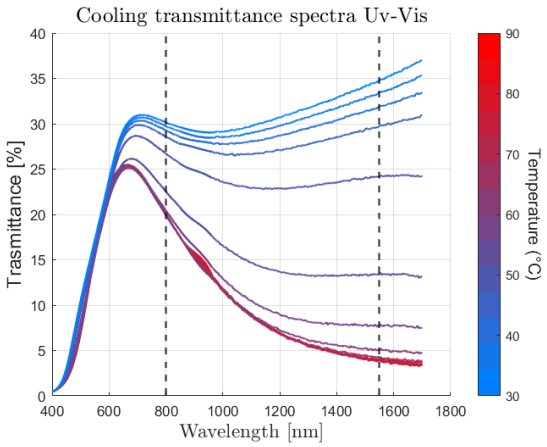

Figure 6.2: Cooling evolution of the transmittance spectra

The resulting heating and cooling hysteresis loops can be fitted with a Complementary Error Function (CEF) with four parameters [3]:

$$f_{\text{CEF}}(x; y_0, A, \mu, \sigma) = y_0 + \frac{1}{2} A \operatorname{erfc}\left(\sqrt{2}\frac{x-\mu}{\sigma}\right) \tag{6.1}$$

where

$$\operatorname{erfc}(x) \equiv 1 - \operatorname{erf}(x) \equiv 1 - \frac{2}{\sqrt{\pi}} \int_0^x dt\, e^{-t^2} \tag{6.2}$$

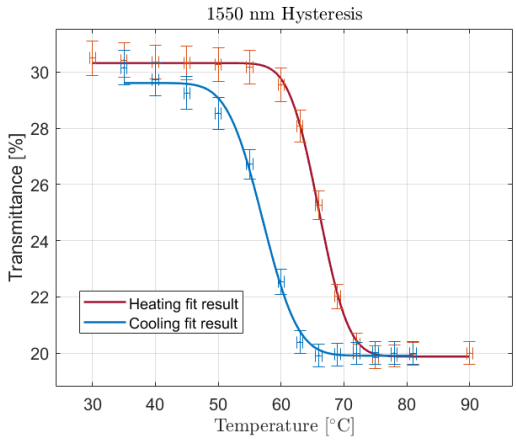

Figure 6.3: Hysteresis cycle at the 1550 nm wavelength.

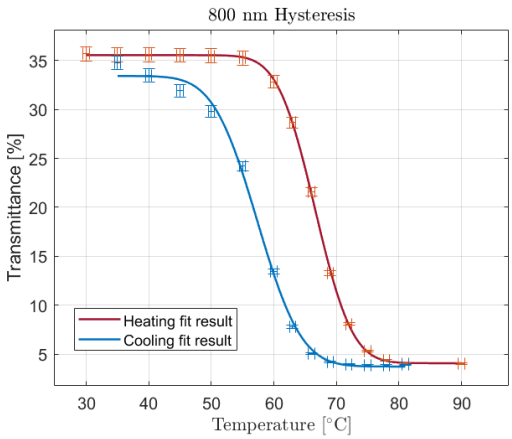

Figure 6.4: Hysteresis cycle at the 800 nm wavelength.

The fit returns the values of the transition temperature μ and the broadening σ for the heating (T_H, σ_H) and cooling (T_C, σ_C) curves, which are reported in Table 6.1. The uncertainty is estimated through error propagation formulas and the temperature error of the heater, which is ± 1°C.

Wavelength [nm]	T_H [°C]	T_C [°C]	σ_H [°C]	σ_C [°C]
1550	67 ± 1	57 ± 1	9 ± 1	11 ± 1
800	66 ± 1	57 ± 1	8 ± 1	9 ± 1

Table 6.1: Comparsion of the fit results for the two wavelengths, T_H and T_c are the heating and cooling transition temperatures respectively, while σ_H and σ_C represent the transition width.

6.2 GIXRD structural hysteresis

A corresponding hysteretic behavior is observed structurally by collecting grazing-incidence X-ray diffraction spectra, focusing on the peak at around 27.9° while cycling the temperature between 30°C and 90°C in 3°C steps.

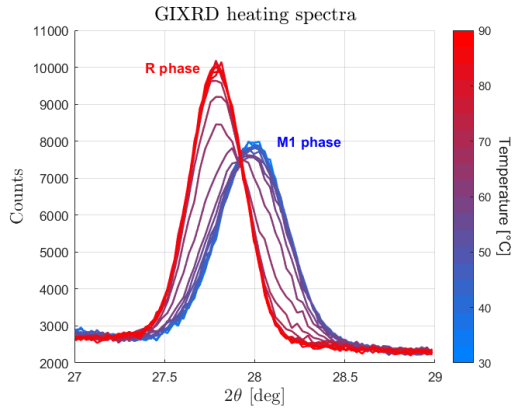

Figure 6.5: Heating evolution of the 27.9° diffraction peak

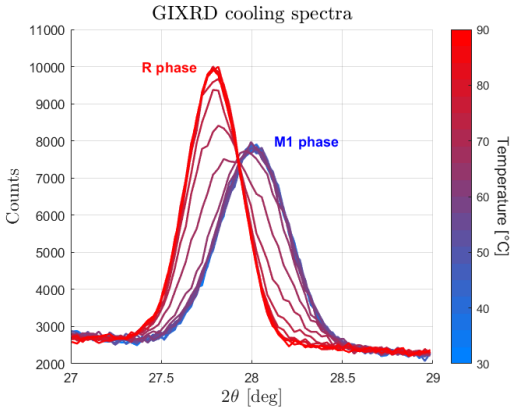

Figure 6.6: Cooling evolution of the 27.9° diffraction peak

The results are reported in Figure 6.5 and 6.6, for the heating and cooling cycle, respectively. The individual diffraction peaks are fitted using a pseudo-Voigt function combined with a linear baseline that accounts for the broad background signal originating from the Silicon substrate.[3] This mathematical approach can track the transition by monitoring the continuous shift of the peak centroid (μ) of the pseudo-Voigt function.

$$f_{\text{pV-lin}}(x; A, y_0, b, \mu, \sigma, w) = y_0 + bx + V_p(x; A, \mu, \sigma, w), \tag{6.3}$$

where

$$\begin{aligned} V_p(x; A, \mu, \sigma, w) = A \left(w \frac{1}{\pi} \frac{2\sigma}{4(x-\mu)^2 + \sigma^2} + \right. \\ \left. + (1-w) \frac{\sqrt{4\ln 2}}{\sqrt{\pi}\sigma} \exp\left[-\frac{4\ln 2}{\sigma^2} (x-\mu)^2 \right] \right). \end{aligned} \tag{6.4}$$

The value of the coefficient μ is reported in the figure below.

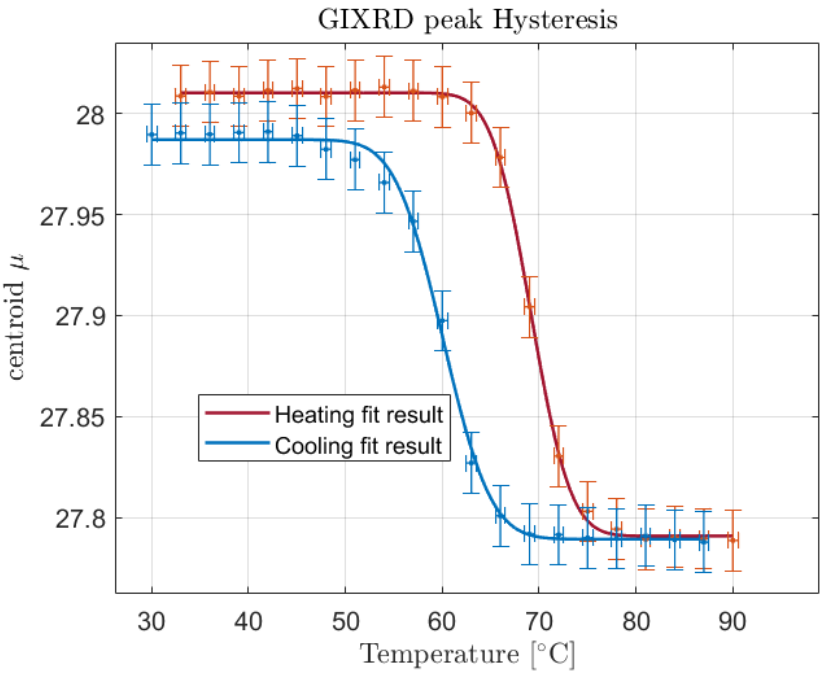

Figure 6.7: Evolution of the 27.9° peak between 30°C and 90°C.

The function used to fit the hysteresis loop is the same CEF used with the spectrophotometer data.

T_H [°C]	T_C [°C]	σ_H [°C]	σ_C [°C]
69 ± 1	60 ± 1	6 ± 1	8 ± 1

Table 6.2: Fit results of the hysteresis cycle, T_H and T_C are the heating and cooling transition temperatures respectively, while σ_H and σ_C represent the transition width.

6.3 Comparison between the two techniques

A direct comparison of the hysteresis cycles obtained with GIXRD and with Optical Transmittance at 1550 nm is shown in Figure 6.8: the two techniques yield very similar results, but with small differences in the transition temperatures, which can be attributed to the following possible causes:

1. Calibration of the two instruments: the heating setup on the spectrophotometer is intrinsically less accurate due to the smaller heated platform and worse contact of the sample compared to the GIXRD. So the difference of about 1-2°C can be attributed to the different accuracy in the calibration: this uncertainty on the temperature could cause a translation of the whole hysteresis curve.

2. Different aspects observed of the VO_2:

   - ◇ The optical spectrometer probes at a relatively smaller area of the sample, effectively averaging the signal response through different grain size areas, composition and stress, while X-rays scan a much larger area, increasing the contribution of local variations.
   - ◇ X-ray diffraction probes the structural (Monoclinic → Rutile) part of the sample, while transmittance is governed by the electronic (Insulator → Metal) part, which can be less sensitive to grain size and/or strain in the sample.

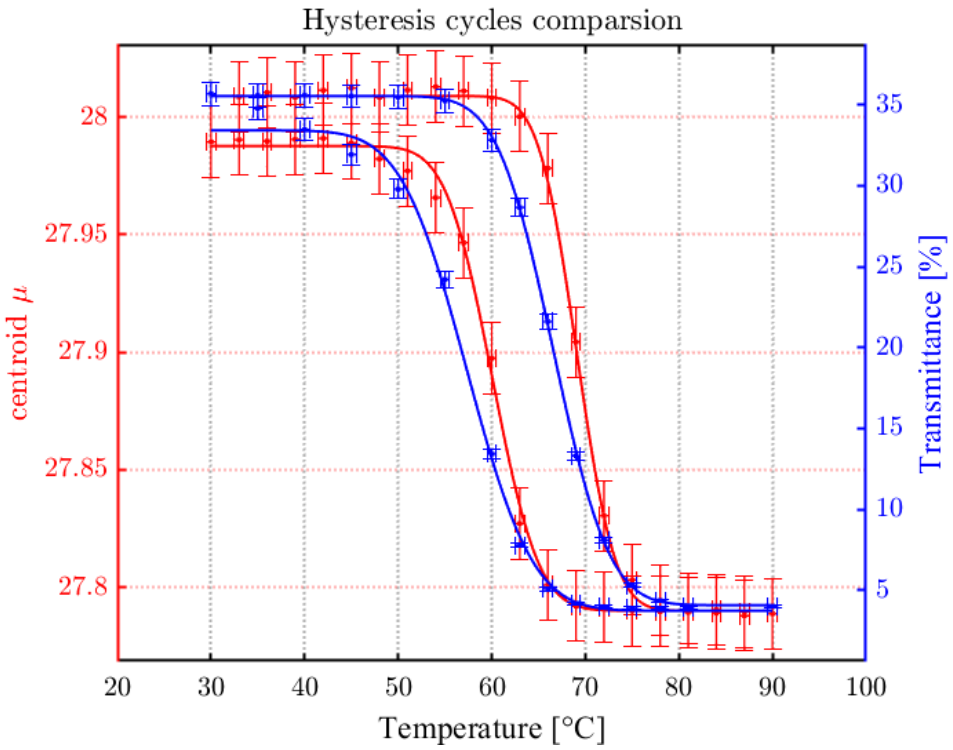

Figure 6.8: Comparsion between the two normalized hysteresis cycles, GIXRD 27.9° peak centroid in red and 1550 nm transmittance in blue

7 Conclusions

The final objective of this thesis was to provide a complete introduction to the world of synthesizing and characterizing an advanced, phase-change material and its properties, to understand how to control them and obtain the desired results. VO_2 was chosen because it is very important for a variety of highly-relevant technological applications. It is also very stimulating as a training ground to employ a variety of different techniques to observe it from different points of view. The first part of the activity involved synthesis via Magnetron Sputtering and thermal annealing, allowing for firsthand observation of the whole process and experiencing the effects of all the different procedures on the final sample. Profilometry measurements and ellipsometry fits showed a final thickness of 125 nm compared to the expected nominal value of 120 nm.

The following step involved morphological characterization, where SEM and AFM microscopy were the perfect techniques to visually and clearly depict the results of the synthesis by obtaining information such as roughness and grain size, which turned out to be 3.1 nm and 52 nm respectively. GIXRD, Raman, and Uv-vis spectroscopies were excellent examples of the practical applications of techniques studied during previous courses, used to obtain structural information on the bonds and crystalline indices, confirming the exclusive presence of VO_2 crystalline oxide phase.

The dielectric function of the sample was determined using ellipsometry, where analyzing the gathered data was a challenge due to the multiple fitting parameters; however, it provided much new knowledge. The MIT transition hysteresis was investigated by observing the sample from both the optical (Transmittance) and structural (GIXRD) points of view, showing the correlation between the two. The first method showed a heating transition temperature of 67°C and a cooling transition temperature of 57°C, while the second method showed 69°C and 60°C. The hysteresis width was broader for the Uv-vis (9°C and 11°C) compared to the GIXRD (6°C and 8°C).

Bibliography

[1] F. J. Morin. "Oxides Which Show a Metal-to-Insulator Transition at the Neel Temperature". In: *Physical Review Letters* 3.1 (July 1959), pp. 34–36. DOI: 10.1103/PhysRevLett.3.34.

[2] Yanqing Zhang, Weiming Xiong, Weijin Chen, and Yue Zheng. "Recent Progress on Vanadium Dioxide Nanostructures and Devices: Fabrication, Properties, Applications and Perspectives". In: *Nanomaterials* 11.2 (Jan. 2021), p. 338. ISSN: 2079-4991. DOI: 10.3390/nano11020338.

[3] Tiziana Cesca, Carlo Scian, Emilija Petronijevic, Grigore Leahu, Roberto Li Voti, Gianmario Cesarini, Roberto Macaluso, Mauro Mosca, Concita Sibilia, and Giovanni Mattei. "Correlation between in situ structural and optical characterization of the semiconductor-to-metal phase transition of VO2 thin films on sapphire". In: *Nanoscale* 12.2 (Jan. 2, 2020), pp. 851–863. ISSN: 2040-3372. DOI: 10.1039/C9NR09024J.

[4] Christian Brahms, Lin Zhang, Xiao Shen, Utso Bhattacharya, Maria Recasens, Johann Osmond, Tobias Grass, Ravindra W. Chhajlany, Kent A. Hallman, Richard F. Haglund, Sokrates T. Pantelides, Maciej Lewenstein, John C. Travers, and Allan S. Johnson. "Decoupled few-femtosecond phase transitions in vanadium dioxide". In: *Nature Communications* 16.1 (Apr. 19, 2025), p. 3714. ISSN: 2041-1723. DOI: 10.1038/s41467-025-58895-z.

[5] Yuanyuan Cui, Yujie Ke, Chang Liu, Zhang Chen, Ning Wang, Liangmiao Zhang, Yang Zhou, Shancheng Wang, Yanfeng Gao, and Yi Long. "Thermochromic VO2 for Energy-Efficient Smart Windows". In: *Joule* 2.9 (Sept. 19, 2018), pp. 1707–1746. ISSN: 2542-4351. DOI: 10.1016/j.joule.2018.06.018.

[6] F. Béteille and J. Livage. "Optical Switching in VO2 Thin Films". In: *Journal of Sol-Gel Science and Technology* 13.1 (Jan. 1, 1998), pp. 915–921. ISSN: 1573-4846. DOI: 10.1023/A:1008679408509.

[7] Kirti Dalal and Yashna Sharma. "Plasmonic switches based on VO2 as the phase change material". In: *Nanotechnology* 35.14 (Jan. 2024), p. 142001. ISSN: 0957-4484. DOI: 10.1088/1361-6528/ad1642.

[8] Chong Wen, Liquan Feng, Zhaohui Li, Jinglian Bai, Shaoyan Wang, Xingxing Gao, Jian Wang, and Wenqing Yao. "A review of the preparation, properties and applications of VO2 thin films with the reversible phase transition". In: *Frontiers in Materials* 11 (Jan. 19, 2024). ISSN: 2296-8016. DOI: 10.3389/fmats.2024.1341518.

[9] Dong-ping Zhang, Mao-dong Zhu, Yi Liu, Kai Yang, Guang-xing Liang, Zhuang-hao Zheng, Xing-min Cai, and Ping Fan. "High performance VO2 thin films growth by DC magnetron sputtering at low temperature for smart energy efficient window application". In: *Journal of Alloys and Compounds* 659 (Feb. 25, 2016), pp. 198–202. ISSN: 0925-8388. DOI: 10.1016/j.jallcom.2015.11.047.

[10] D. Vernardou, M. E. Pemble, and D. W. Sheel. "The Growth of Thermochromic VO2 Films on Glass by Atmospheric-Pressure CVD: A Comparative Study of Precursors, CVD Methodology, and Substrates". In: *Chemical Vapor Deposition* 12.5 (2006). _eprint: https://onlinelibrary.wiley.com/doi/pdf/10.1002/cvde.200506419, pp. 263–274. ISSN: 1521-3862. DOI: 10.1002/cvde.200506419.

[11] Chenxi Zhang, Wei Cao, Adetayo V. Adedeji, and Hani E. Elsayed-Ali. "Preparation and properties of VO2 thin films by a novel sol–gel process". In: *Journal of Sol-Gel Science and Technology* 69.2 (Feb. 1, 2014), pp. 320–324. ISSN: 1573-4846. DOI: 10.1007/s10971-013-3220-5.

[12] I.Y. Forero-Sandoval. "VO_2 Substrate Effect on the Thermal Rectification of a Far-Field Radiative Diode". In: *Physical Review Applied* 14.3 (2020). DOI: 10.1103/PhysRevApplied.14.034023.

[13] Yanjie Cui and Shriram Ramanathan. "Substrate effects on metal-insulator transition characteristics of rf-sputtered epitaxial VO2 thin films". In: *Journal of Vacuum Science & Technology A* 29.4 (May 25, 2011), p. 041502. ISSN: 0734-2101. DOI: 10.1116/1.3584817.

[14] Mian Azmat, Junlin Yang, Haibo Jin, Hajra, Saba Shoaib, Muhammad Kashif Naseem, Qianyi Li, and Jingbo Li. "Optimizing Phase Transition and Thermochromic Performance of Vanadium Dioxide Thin Films via Erbium Doping". In: *ACS Applied Optical Materials* 2.2 (Feb. 23, 2024), pp. 350–360. DOI: 10.1021/acsaom.3c00460.

[15] Yanfei Wu, Lele Fan, Qinghua Liu, Shi Chen, Weifeng Huang, Feihu Chen, Guangming Liao, Chongwen Zou, and Ziyu Wu. "Decoupling the Lattice Distortion and Charge Doping Effects on the Phase Transition Behavior of VO2 by Titanium (Ti4+) Doping". In: *Scientific Reports* 5.1 (May 7, 2015), p. 9328. ISSN: 2045-2322. DOI: 10.1038/srep09328.

[16] O. F. Kolomys, V. V. Strelchuk, P. M. Lytvyn, D. M. Maziar, V. M. Dzhagan, and O. V. Dubikovskyi. "Raman and scanning spreading resistance mapping of the evolution of structural phases near the insulator–metal transition in VO2 films". In: *Applied Surface Science* 715 (Jan. 15, 2026), p. 164627. ISSN: 0169-4332. DOI: 10.1016/j.apsusc.2025.164627.

[17] Boris Kalinic, Tiziana Cesca, Alessandro Lovo, Carlo Scian, Roberto Macaluso, Fabio Bovino, Roberto Li Voti, Concita Sibilia, and Giovanni Mattei. "Active Modulation of Er3+ Emission Lifetime by VO2 Phase-Change Thin Films". In: *Advanced Photonics Research* 5.2 (2024), p. 2300242. ISSN: 2699-9293. DOI: 10.1002/adpr.202300242.

[18] *Materials Project*. Materials Project. URL: https://next-gen.materialsproject.org/materials/mp-1102963?formula=VO2 (visited on 05/25/2026).

[19] None Available. *Materials Data on VO2 by Materials Project*. In collab. with The Materials Project. 2020. DOI: 10.17188/1193879.

[20] Yan Yang, Xun Cao, Guangyao Sun, Shiwei Long, Tianci Chang, Xiaozhe Li, and Ping Jin. "Transmittance change with thickness for polycrystalline VO2 films deposited at room temperature". In: *Journal of Alloys and Compounds* 791 (June 30, 2019), pp. 648–654. ISSN: 0925-8388. DOI: 10.1016/j.jallcom.2019.03.278.

[21] Rama Satya Sandilya V., Arvind Rajnarayan Singh, Sandeep Vura, Shubham Kumar Parate, Anirudh Venugopalarao, Srinivasan Raghavan, Pavan Nukala, and Sushobhan Avasthi. "Texture and phase transition hysteresis in epitaxially integrated VO2 films on TiN/Si(100)". In: *Materialia* 34 (May 1, 2024), p. 102085. ISSN: 2589-1529. DOI: 10.1016/j.mtla.2024.102085.

Acknowledgments

I would like to thank the Department of Physics at the University of Padova for providing the necessary spaces and equipment to complete this thesis project. In particular, I would like to mention my supervisor, Professor Giovanni Mattei, for his great expertise in this field and the willingness to support me in the project. I would also like to include the department staff, including Carlo Scian, Enrico Lanaro, Boris Kalinic, and Ilaria Debono, who taught me how to use the equipment and provided me with invaluable tips. I would like to thank my parents and my family for supporting me in all possible aspects since the day I decided to pursue this Bachelor's degree. Finally, I would also like to mention my friends and student colleagues who played a big role in sharing the highs and lows of these three amazing years; without them, this journey wouldn't have been the same.